Developmental Cognitive Neuroscience 20 (2016) 2–11

Contents lists available at ScienceDirect

Developmental Cognitive Neuroscience

journal homepage: http://www.elsevier.com/locate/dcn

Connectome hubs at resting state in children and adolescents: Reproducibility and psychopathological correlation

João Ricardo Sato[a,c,g,h,*], Claudinei Eduardo Biazoli Jr[a,g], Giovanni Abrahão Salum[b,h], Ary Gadelha[c,h], Nicolas Crossley[f,i], Gilson Vieira[e,g], André Zugman[c,h], Felipe Almeida Picon[b,h], Pedro Mario Pan[c,h], Marcelo Queiroz Hoexter[c,d,h], Mauricio Anés[b,h], Luciana Monteiro Moura[c,h], Marco Antonio Gomes Del'Aquilla[c,h], Edson Amaro Junior[g], Philip Mcguire[f], Luis Augusto Rohde[b,h], Euripedes Constantino Miguel[d,h], Rodrigo Affonseca Bressan[c,h], Andrea Parolin Jackowski[c,h]

[a] Centro de Matemática, Computação e Cognição, Universidade Federal do ABC, Santo Andre, Brazil
[b] Department of Psychiatry, Federal University of Rio Grande do Sul and Psychiatric Service, Hospital de Clinicas de Porto Alegre, Brazil
[c] Interdisciplinary Lab for Clinical Neurosciences (LiNC), Universidade Federal de Sao Paulo (UNIFESP), Sao Paulo, Brazil
[d] Department of Psychiatry, University of São Paulo School of Medicine, São Paulo, Brazil
[e] Bioinformatics Program, Institute of Mathematics and Statistics, University of Sao Paulo, Brazil
[f] Institute of Psychiatry, King's College London, United Kingdom
[g] Department of Radiology, School of Medicine, University of Sao Paulo, Brazil
[h] National Institute of Developmental Psychiatry for Children and Adolescents, CNPq, Brazil
[i] Institute for Biological and Medical Engineering, Faculties of Engineering, Medicine and Biological Sciences, P. Catholic University of Chile, Chile, Chile

ARTICLE INFO

Article history:
Received 2 December 2015
Received in revised form 9 May 2016
Accepted 9 May 2016
Available online 14 May 2016

Keywords:
Resting state
Replication
fMRI
Connectivity
Development
Children

ABSTRACT

Functional brain hubs are key integrative regions in brain networks. Recently, brain hubs identified through resting-state fMRI have emerged as interesting targets to increase understanding of the relationships between large-scale functional networks and psychopathology. However, few studies have directly addressed the replicability and consistency of the hub regions identified and their association with symptoms. Here, we used the eigenvector centrality (EVC) measure obtained from graph analysis of two large, independent population-based samples of children and adolescents (7–15 years old; total N = 652; 341 subjects for site 1 and 311 for site 2) to evaluate the replicability of hub identification. Subsequently, we tested the association between replicable hub regions and psychiatric symptoms. We identified a set of hubs consisting of the anterior medial prefrontal cortex and inferior parietal lobule/intraparietal sulcus (IPL/IPS). Moreover, lower EVC values in the right IPS were associated with psychiatric symptoms in both samples. Thus, low centrality of the IPS was a replicable sign of potential vulnerability to mental disorders in children. The identification of critical and replicable hubs in functional cortical networks in children and adolescents can foster understanding of the mechanisms underlying mental disorders.

1. Introduction

Graph theory has been increasingly applied in the analysis of connectivity in neuroimaging data. Graph-theory-derived centrality measures, especially eigenvector centrality (EVC), can rank the relevance of a node in a complex network (Zuo et al., 2012) in terms of strategic location. This feature is particularly useful for exploring the etiology of mental disorders that are associated with functional alterations at a network rather than a focal level (Fornito et al., 2015; Sporns, 2014; He et al., 2016). However, there is currently a lack of consistent findings from independent large samples in the literature (Horga et al., 2014). In particular, few studies have investigated if central functional brain regions in children and adolescents are replicable across different sites of acquisition (Zuo et al., 2012). In addition, even fewer studies have explored the

* Corresponding author at: Av. dos Estados, 5001, Bairro Bangu, Santo André, SP CEP 09210–580, Brazil.
E-mail address: joao.sato@ufabc.edu.br (J.R. Sato).

http://dx.doi.org/10.1016/j.dcn.2016.05.002

replicability of associations between network-level disruptions and dimensional psychopathology in childhood.

Previous studies of human structural and functional brain networks have identified a set of highly connected brain regions (i.e., hubs) (Power et al., 2013). These hubs are believed to play a central role in the flow of information throughout the brain, integrating parallel and distributed networks (Gong et al., 2009; Hagmann et al., 2008; Hwang et al., 2013). Structural connectivity studies have shown that hubs are mainly located at integrative cortical areas in adults (Power et al., 2013; Sporns et al., 2007). In the adult brain, functional cortical hubs include the medial prefrontal cortex, posterior cingulate cortex (PCC), precuneus, inferior parietal lobule (IPL; particularly the angular gyrus) and medial temporal cortex (Buckner et al., 2009). Moreover, Betzel et al. (2014) have noted that functional hub regions are affected by changes in white matter connections and that the relationship between functional and structural connectivity changes with age.

Two major gaps can be drawn from the current neuroimaging literature of children and adolescents: (i) the replicability across different samples; and (ii) the differential effects of hubs over neurodevelopment. Several resting-state fMRI studies of large samples of children and adolescents have been carried out, but in healthy developing children as opposed to clinical samples (Grayson et al., 2014; Sato et al., 2015a,b; Supekar et al., 2009; Uddin et al., 2011; Hwang et al., 2013). Evidence for a typical developmental trajectory emerged from these studies: large-scale networks apparently shift from a locally segregated to a more distributed and integrated organizational pattern (Fair et al., 2008, 2009, 2007; Fransson et al., 2011; Gao et al., 2009; Supekar et al., 2009). Interestingly, in infants, hubs have been identified in primary sensorimotor regions as opposed to the association cortex, where hubs have been identified in adults (Fransson et al., 2011). Hwang et al. (2013) showed that the connectivity between frontal hubs and other brain regions increases from childhood to adolescence. However, Khundrakpam et al. (2013) described developmental changes in the topological properties of the networks that suggested an organizational shift towards a more random configuration. Moreover, Zuo et al. (2012) demonstrated the test-retest reliability of EVC in functional connectivity networks over a subject age range of 7–85 years old. Therefore, despite the emergence of several brain regions as potential hubs of intrinsic brain connectivity in children, few studies have investigated which regions are most replicable across different samples (Horga et al., 2014). This is a crucial point for progress in biological psychiatry. In addition, many findings from early resting-state fMRI studies were limited by the issue of head micro-motion artifacts (Power et al., 2012). These movement artifacts are also related to age and influence functional connectivity estimates, complicating the interpretation of results.

The fact that hub regions constitute potential points of vulnerability for network disintegration is a key issue (Albert et al., 2000). Indeed, the abnormalities associated with several brain disorders have been shown to concentrate in hubs; such disorders include ADHD (dos Santos Siqueira et al., 2014), autism (Ray et al., 2014) and schizophrenia (Tomasi and Volkow, 2014). As such, hub disruption has been proposed as a general pathological mechanism in brain disorders (Crossley et al., 2014; van den Heuvel and Sporns, 2013). Therefore, description of atypical neurodevelopmental trajectories of the brain connectome appears crucial to unveil the neural substrates of mental symptoms and disorders (Di Martino et al., 2014). However, full characterization of these functional networks and possible differences in their architecture in childhood has not yet been achieved.

Here, we first sought to explore the replicability of mapping regions with high EVC values in children and adolescents. Then, we investigated the hypothesis that diminished or "impaired" centrality of these hubs would reliably correlate with psychopathological symptoms in two independent, population-based cohorts of children and adolescents. For these purposes, we analyzed resting-state fMRI data acquired using identical acquisition protocols from two large samples of children and adolescents who were recruited at two different centers in Brazil.

2. Materials and methods

2.1. Subjects

The children and adolescents who participated in this study were part of the '*High Risk Cohort Study for Psychiatric Disorders in Childhood*' (HRC, N = 2512 children; for a detailed description see Salum et al., 2013, 2014). This is a population-based sample of children from among the 9937 students of 57 public schools in two Brazilian cities: São Paulo (site 1) and Porto Alegre (site 2). The members of the HRC cohort were screened using a modified version of the Family History Screen (Weissman et al., 2000). Nine hundred fifty-eight subjects were randomly selected, and 1554 were selected based on their risk of developing psychiatric disorders (using the same criteria at the two sites; Salum et al., 2013, 2014); these individuals comprised the 2512 subjects of the HRC.

Among the total of 2512 volunteers, 741 subjects (and their parent/guardian) accepted the invitation for MRI scanning session. Functional MRI data were acquired from these subjects using the same acquisition protocol at the two sites. Eighty-nine participants were discarded due to an incomplete session, missing data, observable excessive motion (as identified by the system operator) or preprocessing errors (failure in registration to the template/atlas).

Thus, 652 remaining subjects were considered in the analyses of the current study. Because this was a community sample, participants were not discarded depending on IQ. The mean age (years) ± standard deviation (sd) of the participants was 10.81 ± 2.00 at site 1 and 10.58 ± 1.75 at site 2, with ages ranging from 7 to 15 years at both sites. Three hundred forty-one subjects were scanned at site 1 (165 males, 159 randomly selected) and 311 at site 2 (179 males, 139 randomly selected).

The local ethics committee approved this study. Written consent was obtained from all of the parents (or legal guardians), and verbal assent was obtained from all of the participants.

2.2. Assessment

IQ was estimated using the vocabulary and block design subtests of the Wechsler Intelligence Scale for Children (in a household interview) and the approach of Tellegen and Briggs (1967). The socioeconomic status of the families was classified according to the Brazilian rating scale (ABIPEME, 2010; low = E and D classes; medium = C and B classes; high = A class):

The parents/caregivers filled out a Portuguese-translated version of the Child Behavior Checklist (CBCL) (Achenbach and Rescorla, 2001) on the day of scanning. This assessment tool provided scores for psychopathological manifestations. The total CBCL score is a measure of overall psychopathology. It represents the sum of points for 112 CBCL items (0, 1 and 2 points per item), including the 8 syndromes described by the questionnaire (anxiety/depression, withdrawal/depression, somatic, rule breaking, aggression, social problems, thought problems and attention problems) as well as other symptoms not classified with any syndrome. The total CBCL score is a common measure of overall psychopathology. The analyses were carried out only for the total CBCL scores and not for scores on all the subscales to reduce the number of multiple comparisons and because the subscale scores are highly correlated with low specificity.

2.3. Data acquisition

Recreational activities were performed for desensitization on the day of scanning. The neuroimaging data were acquired using two 1.5 T MR systems (Signa HDX and HD from the same manufacturer—G.E., United States of America) using the same parameters and protocols. The fMRI acquisition protocol consisted of 180 EPI dynamic volumes with the following parameters: TR = 2000 ms; TE = 30 ms; slice thickness = 4 mm; gap = 0.5 mm; flip angle = 80°; matrix size = 80 × 80; reconstruction matrix = 128 × 128, 1.875 × 1.875 mm; NEX = 1; number of slices = 26; and total acquisition time = 6 min. Resting-state scans were acquired while the subject's eyes were open and fixated on a target. Alongside the functional images, T1-weighted scans (3D FSPGR sequence) were collected to cover the whole brain, up to 160 axial slices (TR = 10.91 ms; TE = in phase 4.2 ms; thickness = 1.2 mm; flip angle = 15°; matrix size = 256 × 192; FOV = 24.0 × 18.0 cm; and NEX = 1).

2.4. Data preprocessing

The neuroimaging data were preprocessed using AFNI (version 2011_12_21_1014) (Cox, 1996) and FSL software (version 5.0) (Jenkinson et al., 2012). We used the following steps (scripts from www.nitrc.org/projects/fcon_1000): discarding of the first four volumes of EPI; skull stripping; head motion correction; despiking; rescaling to a grand mean of 10000; band-pass filtering (0.01 and 0.1 Hz); detrending; spatial smoothing (FWHM = 8 mm); linear registration to the subject's structural scan; structural image non-linear registration to the Montreal Neurological Institute (MNI152) template; non-linear registration of functional scans; and regression out of nuisance covariates (CSF, white matter, global signal and six linear motion parameters). The scrubbing method proposed by Power et al. (2012) was applied to minimize the impact of head motion. Scans (frames) were discarded (flagged frame as well as one before and two after) if the corresponding frame-wise displacement (FD) or the temporal derivative of the RMS variance over the voxels (DVARS) was greater than the 95th percentile of all subjects with successful processing (FD > 0.5 mm and DVARS > 46.4).

2.5. Network modeling

For each subject, the average BOLD signal was extracted from 325 similarly sized regions of interest covering the whole brain (Patel et al., 2014); these ROIs were defined using previously established algorithms (Zalesky, 2011). Although some notable studies (Zuo et al., 2012) have used a voxel-wise approach to construct connectomes, we opted to use a ROI-based approach for two main reasons: (i) voxel-wise analyses would considerably increase the positive correlations between regions due to spatial smoothing and data redundancy; and (ii) the number of comparisons in subsequent statistical testing would be increased from the order of hundreds to tens of thousands. A pairwise Pearson correlation was calculated between every pair of ROIs, and these correlations were then used to index the strength of functional connectivity.

A graph is a mathematical object that can be used to represent networks in general (social, brain, transport networks, etc.). This representation facilitates the extraction of some descriptive features and quantitative analyses. In the current study, the ROIs are the graph nodes, and edges represent the functional connectivity between them. To avoid arbitrary choices of functional connectivity, we modelled an undirected weighted graph by using the absolute value of the Pearson correlation coefficients as the weight of the connections. This approach has some limitations because it considers correlated and "anti-correlated" networks in the same manner, which may make interpreting this graph from a physiological perspective difficult. We discuss this limitation in the Discussion section. In addition, short-distance correlations might be affected by spatial smoothing, slicing and head movement (Grayson et al., 2014; Power et al., 2013); thus, we discarded connections between ROIs that were less than 20 mm apart.

The EVC of a node is a metric obtained from graph analysis that quantifies the relevance of a node (i.e., a brain region in this case) in the context of the organization of connections of the network. In other words, some nodes interact with the whole network more than others, and these key nodes are named hubs. Thus, to investigate the hierarchical organization of the whole-brain network, we ranked all of the included ROIs according to their EVC. The EVC of a brain region is proportional to the EVC of its connected regions (Bonacich, 1987). In this sense, EVC also considers how the neighbors (connected regions) of a node are connected to the network. This is a well-established method in graph analysis that is used to investigate the hierarchical relevance of a node, or its 'hubness', in the context of the global features of a network (Rubinov and Sporns, 2010). For each subject, the EVC of the nodes was calculated by the eigenvector corresponding to the greatest eigenvalue of the correlation matrix (in absolute values) between the BOLD signal of the ROIs (i.e., if **A** is the bivariate correlation matrix, the EVC is the vector x such that **A**x = mx, for the greatest m).

In the current study, we focused solely on EVC as the metric used to identify hubs for the following reasons: (i) EVC provides a global measure of centrality that takes into account not only the neighbors of a node but also the context of the whole network; (ii) this metric is based on connection strength (weights) and not distance (and is thus a straightforward choice regarding functional connectivity. Otherwise, a distance metric based on correlations must be defined); (iii) EVC displays good test-retest reliability, as demonstrated by Zuo et al. (2012), and is sensitive for functional connectivity changes in children and adolescents (Sato et al., 2015a,b); and (iv) exploring other centrality measures would at least double the number of comparisons.

2.6. Data analysis

We analyzed each site of acquisition separately, which allowed us to assess the reliability of our analyses across the two samples. We first calculated the mean EVC rank across subjects for every ROI. Subsequently, we identified the overlap (across sites) of the top 10% (21 out of 325) of regions with the highest EVC ranks. Then, a Monte Carlo analysis was performed to assess the significance of the number of overlapping regions, preserving the correlation structure between regions at each site. Finally, to demonstrate that the replicability across sites was not dependent on the 10% threshold, we also repeated the overlap analyses for the regions with EVC ranks within the top 5% and top 1%.

Once these top 10% EVC hub regions were identified, we tested the hypothesis that the subjects with hubs with lower EVC ranks would be more likely to have psychiatric symptoms. For each region (from 21 hubs), a univariate general linear model (GLM) was fitted, considering the total CBCL score as the dependent variable; the EVC rank as the main regressor; and gender, age and degree of head motion (measured by the mean FD) as nuisance variables. Although EVC was the main variable of interest, the nuisance variables – mainly FD – were included as covariates not to assess their significance but to take them into account as potential confounders. Moreover, to reduce the number of comparisons, we excluded brain regions with suspected influences of head motion. The 21 GLMs were also performed without FD as a covariate. Thus, the brain regions for which the EVC p-value difference (with and without FD as a covariate) was greater than 5% were excluded from results. The Type I error for the remaining regions was set at 5% (uncorrected for multiple comparisons).

3. Results

Fig. 1 highlights a strong replication (Pearson's r = 0.91, p < 0.001) of the ranks of the mean EVC (across subjects) for brain regions in the two sites, especially for regions with high and low EVC values; more variability was observed in the intermediate values. Our main result was the overlap (across sites) of 21 regions within the set of regions with EVC scores within the top 10% (see Table 2). For the top 5% and 1%, the number of overlapping regions was 11 and 2, respectively. The *p*-value for the comparison of the number of overlapping regions was less than 0.001 (Monte Carlo method), regardless of the threshold (10%, 5% and 1%) considered.

As shown in Fig. 2, the individual variability in the EVC scores of the overlapping regions was relatively low, with similar results for both sites. Fig. 3 shows brain maps of the hub regions that overlapped across the sites. Note that regardless of the threshold considered, the anterior medial prefrontal cortex (amPFC) and the IPL/intraparietal sulcus (IPS) were included among the most relevant regions.

Regarding the GLM analyses of psychopathological manifestations, only four regions were not strongly affected by the inclusion of head motion (FD) as a covariate (Table 3). Among these four regions, the EVC rank of the right intraparietal cortex (see Fig. 4) was found to be negatively associated with the CBCL score, a finding replicated at both sites (uncorrected p < 0.02 and 0.03 for site 1 and site 2, respectively). The box plots presented in Fig. 4 (bottom) were built considering a quartile categorization of the mean EVC rank (low if less than first quartile; high if greater than third quartile; typical otherwise). The data were categorized this way solely for visualization purposes (the statistical evaluation was carried out previously through a GLM in which EVC was considered as a quantitative variable) because the association effect is more evident in box plots than in scatter plots.

Regarding head motion, the mean FD (± sd) was 0.19 (±0.29) for site 1 and 0.12 (±0.12) for site 2. As expected, the EVC of the top 10% of regions was significantly correlated (Pearson correlation) with the mean FD. However, the Pearson correlation between mean FD and CBCL score was not significant (p = 0.40 and 0.21 for site 1 and 2, respectively). In addition, we repeated both the hub identification and CBCL analyses by considering only the subjects with a mean FD < 0.2 mm. Only one of the previous 21 regions was not identified as a replicable hub (the right Insula). The results of the CBCL analysis remained the same (see Supplementary Table S1 in the online version at DOI: 10.1016/j.dcn.2016.05.002 for further details). We did not find any significant association between EVC and estimated IQ in either of the two sites. Finally, the findings were not altered by the inclusion of socioeconomic status (SES) as an additional nuisance variable in the GLM analyses (Supplementary Table S2 in the online version at DOI: 10.1016/j.dcn.2016.05.002).

4. Discussion

As integrative nodes, brain hubs play a key role in functional connectivity networks. In the current study, we used two large and independent population-based samples of children and adolescents to explore the consistency of the identification of brain hubs under resting-state conditions and the associations of these hubs with psychopathological symptoms. We first identified a set of hubs that was replicated across both sites: the amPFC and the IPL/IPS. Within this set of hubs, we found that a right IPS with lower EVC was associated with the presence of psychiatric symptoms, a finding that was replicable across the two samples.

In addition to the IPL/IPS and amPFC, other fairly consistent regions (across gender and age) included the ventral medial prefrontal cortex (vmPFC), medial temporal gyrus (mTG), precuneus and PCC. Many of these regions are components of the default mode network (DMN) (Raichle et al., 2001; Raichle and Snyder, 2007). The IPL/IPS and amPFC are associative areas and might play a role as hubs in the cross-modal integration of cortical and subcortical regions (Buckner et al., 2008). The amPFC is involved in social cognition (Wang and Hamilton, 2014), metacognitive abilities for memory and perception (Baird et al., 2013), evaluative judgment and self-referential processes (Zysset et al., 2003). The IPS/IPL is part of the parietal cortex (Rademacher et al., 1992), which has been characterized as a cross-modal hub of multisensory information convergence (Seghier, 2013) and implicated in several cognitive processes. Semantic processing and complex language functions frequently activate the angular gyrus, for instance (Binder et al., 2009; Vigneau et al., 2006). In addition, the right IPL is also involved in attentional maintenance, the encoding of salient events (Singh-Curry and Husain, 2009), spatial cognition, internal representations (Sack, 2009), social cognition (Buckner et al., 2008) and the autobiographical memory system (Spreng et al., 2009). Thus, our findings support crucial roles for the IPL/IPS and amPFC as integrative regions.

From a network dynamics perspective, the amPFC is part of the midline core components of the DMN and may underlie the evaluation of experiences with a high personal significance (Andrews-Hanna et al., 2010). In a detailed study of the structural and functional changes that occur in the DMN, Supekar et al. (2010); Sato et al. (2015a,b) showed that the connectivity between the amPFC and PCC is immature in children. Our finding of a relative absence of the PCC from the group of the most consistent hub regions, in contrast to the amPFC, may be in line with this previous observation. Similarly, the IPS and IPL are central integrative nodes of the frontoparietal component of the executive control network (Dosenbach et al., 2007) and are thought to underlie top-down control. Our results support a view in which the IPL/IPS and amPFC constitute a stable (across the age range investigated) and replicable core of the control/default mode network, with the PCC/precuneus and other parts of the medial prefrontal cortex included as hubs.

Finally, we tested the hypothesis of an association between the disruption of hub regions and the expression of psychiatric symptoms in children and adolescents. As expected, lower values of centrality in a replicable hub region, the right IPS, correlated with the increased expression of psychiatric symptoms. Higher right IPS activity was previously found to be positively correlated with better executive function among populations at risk for brain disorders including mild cognitive impairment (Jacobs et al., 2012) and among carriers of genes associated with predisposition to Parkinson's disease (Thaler et al., 2013). Moreover, right IPS activity was correlated with reduced symptom severity in a subgroup of patients with schizophrenia (Bleich-Cohen et al., 2014). This finding demands further investigation of the potential role of hub impairment, particularly of right IPS, as a potential marker of vulnerability or as part of the natural history of several neuropsychiatric pathologies.

Interestingly, in addition to the correlation of lower EVC values in the right but not left IPS with psychiatric symptoms, the majority of hubs identified were concentrated in the right hemisphere. Higher connectivity and centrality of the right but not the left IPS was previously shown to be associated with improved executive task performance (Markett et al., 2014; Seeley et al., 2007). Furthermore, there is evidence for asymmetric arrangements of large-scale networks, including the DMN (Saenger et al., 2012). By simultaneously acquiring EEG and fMRI, Biazoli et al. (2013) showed that BOLD activity in the nodes of resting-state networks is correlated with an increased flow of information from the right to the left hemisphere. Accordingly, stronger connectivity was found in the

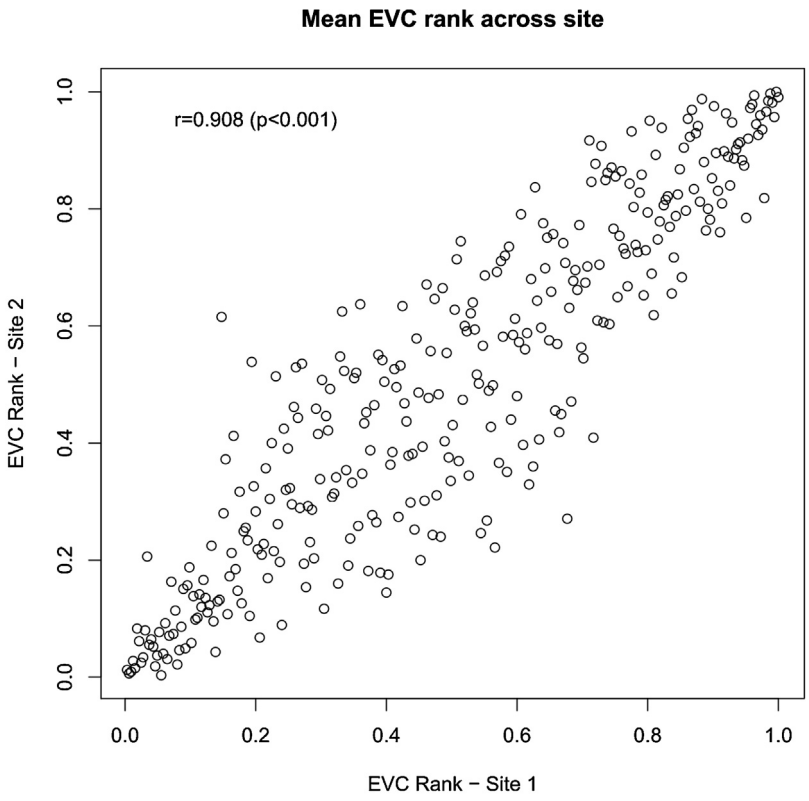

Fig. 1. Scatter plot and Pearson correlation analysis of the mean EVC ranks (of each brain region) between the two sites.

Table 1
Demographical information in each site. The *p*-values comparing the two sites were obtained by using two-sample *t*-tests (unequal variances) for continuous variables and Pearson chi-square tests for SES, handedness and gender.

	Site 1	Site 2	p-value
N	341	311	
age (y.o., mean ± s.d.)	10.81 ± 2.00	10.58 ± 1.75	0.107
Gender	165 (48.39%) males	179 (57.56%) males	0.024
IQ	101.70 ± 16.65	103.42 ± 16.69	0.190
handedness	287 (84.16%) R	269 (86.50%) R	0.884
CBCL total	56.45 ± 32.25	37.67 ± 25.50	<0.001
socieconomic-status (SES)			0.576
high	94 (27.57%)	95 (30.55%)	
medium	231 (67.74%)	205 (65.92%)	
low	16 (4.69%)	11 (3.54%)	
Frame Displacement (F.D)			
mean F.D. pre-scrubbing	0.19 ± 0.29	0.12 ± 0.12	<0.001
mean F.D. post-scrubbing	0.08 ± 0.03	0.08 ± 0.03	1
Scrubbed frames	26.94 ± 38.83	16.47 ± 28.53	<0.001

right hemisphere, and causality measures suggested a crucial functional role of this hemisphere during the resting state (Medvedev, 2014).

Fig. 3 highlights the replicated hubs in yellow, while the regions depicted in red and green show the non-overlapping regions. Some of these regions are nodes of the DMN, such as precuneus/posterior cingulate and right temporal gyrus. In these cases, we believe the divergence between the two sites may be due to sampling fluctuations. In addition, occipital and cerebellar regions seem to be specific to one of the sites. Indeed, although the age and gender distributions were similar between the two sites, the two samples considerably differed in terms of psychiatric symptoms and levels of head motion, as shown in Table 1 . The participants at site 1 presented a wider range of symptom severity and head motion, which may explain the between-sites differences in brain hubs Tables 2 and 3.

Finally, it is important to mention some of the limitations of the current study. Although we used a scrubbing method, head motion artifacts may still affect the analyses. This is an inherent challenge in neuroimaging studies involving children, and the challenge is even greater when psychiatric symptoms are present. We also tried to include FD as a possible confounder in the GLM and discarded regions in which the *p*-value depended on FD. However, head motion effects cannot be completely eliminated because these artifacts may also be due to non-linear influences of motion on the signal or field inhomogeneity. Despite reducing the number of comparisons by discarding the analyses more prone to motion effects, the remaining four GLM analyses with CBCL were not adjusted for multiple testing. Although the findings did not persist after Bonferroni correction, the association between EVC and CBCL in the IPS was replicated across the two sites when uncorrected *p*-values were considered. In addition, we acknowledge that by using the absolute values of the correlation coefficients as functional connectivity estimates, we could not differentiate correlated and "anti-correlated" (negatively correlated) networks. This assumption may not be an accurate representation of the underlying neurophysiology, which may complicate the interpretation of the results. We acknowledge that this approach is not optimal, but there is no established framework (conceptual and methodological) for handling anti-correlated networks in whole-brain analyses. When analyzing these data considering solely the positive correlations between the ROIs, the results are very different because the graph connectivity structure is altered. However, two of the main resting-state networks are the default-mode and control networks (which were part of our findings). Because the activities of both networks are negatively correlated, using solely the connections with positive weights to define the graphs would mask this antagonism. Moreover, some studies suggest that this opposition is intrinsic, and the dynamic of cognitive control involves the union of both systems (Fox et al., 2005; Hellyer et al., 2014). Finally, we emphasize that one of the main limitations of the current study was the

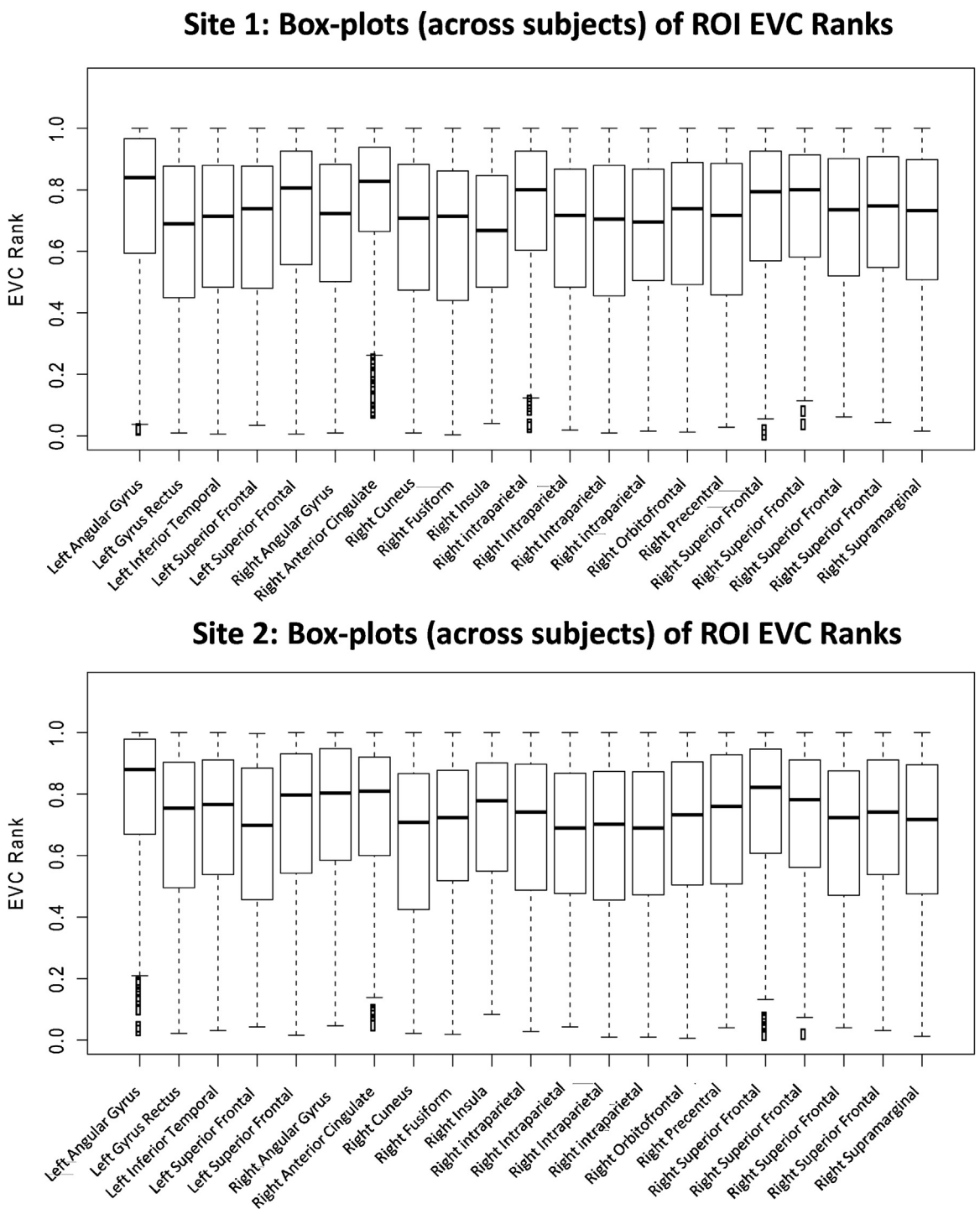

Fig. 2. Analysis of inter-subject variability—Box plots (across subjects) of the EVC ranks (within each site) of the 21 ROIs, separated by site. The ROIs are the brain regions with mean EVC ranks within the top 10% and for which this high centrality was replicated at the two sites of acquisition. The coordinates of these brain regions are described in Table 2.

choice of parcellation scheme. Indeed, the results are expected to vary according to the parcellation atlas used because atlases differ with respect to the number of ROIs and the size and location of the parcels. These differences strongly impact the estimated functional connectomes. We opted to use an anatomical parcellation based on predefined cortical and subcortical areas, but we recognize this is an arbitrary choice.

In summary, our findings suggest that in late childhood and adolescence, the amPFC and IPL/IPS play a role as integrative regions with high hierarchical positions within the whole-brain network. Furthermore, we showed that disruptions in the hierarchical position of the IPS are associated with psychopathology. These results point towards a model in which psychopathological manifestations are associated with disruptions of the typical functional hierarchy of brain networks. Our findings are in agreement with current hypotheses regarding the relationships between mental disorders and abnormal connectomics (Fornito et al., 2015; Satterthwaite and Baker, 2015; Sporns, 2014). Because this study is based on

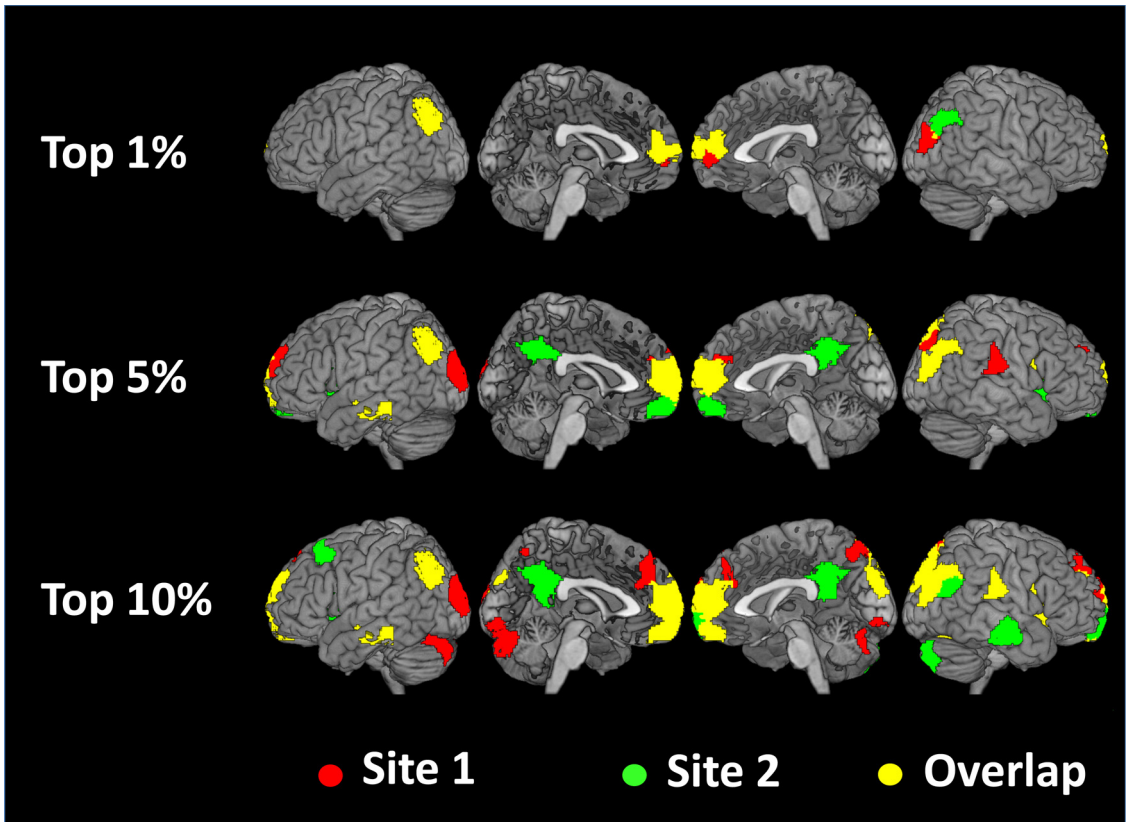

Fig. 3. Brain regions with the top mean EVC scores across the two sites. Overlapping regions are highlighted in yellow. The anterior medial prefrontal cortex (superior frontal) and IPL/IPS were consistently included among the regions with the top centrality ranks.

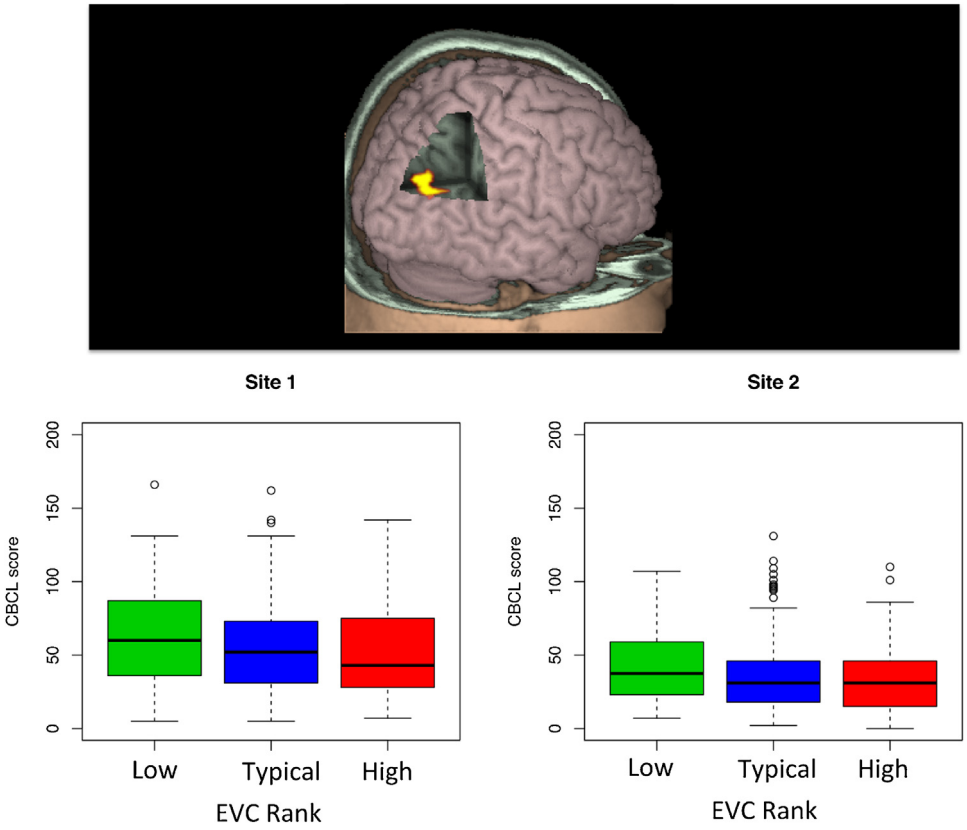

Fig. 4. Association between EVC of the intraparietal cortex and psychiatric symptoms—Brain map depicting the intraparietal cortex ROI (top) and the significant association between its EVC rank and the symptom score (bottom), which was replicated across the two sites.

Table 2
Brain regions included in the top 10% EVC set, replicated across the two sites of acquisition. The regions in the top 5% and 1% EVC sets are highlighted on the right.

Brain Region	MNI − Coordinates (center of mass)			# voxels	top 5%	top 1%
	X	Y	Z			
Left Angular	−44.89	−66.46	38.51	710	*	*
Left Gyrus Rectus	−3.38	55.82	−15.44	713		
Left Inferior Temporal Cortex	−59.87	−24.24	−16.54	598	*	
Left Superior Frontal Cortex	−18.17	57.93	23.89	803		
Left Superior Frontal Cortex	−5.16	65.27	19.25	525	*	
Right Angular	47.13	−65.62	33.81	696	*	
Right Anterior Cingulum	−1.89	51.29	12.15	856	*	*
Right Cuneus	4.68	−87.43	31.42	453		
Right Fusiform	29.6	−63.76	−13.68	709		
Right Insula	40.39	20.35	3.51	877		
Right Occipital Cortex	35.32	−81.47	16.88	864	*	
Right Intraparietal Cortex	34.05	−75.68	29.36	419		
Right Occipital Cortex	19.78	−90.67	26.05	451		
Right Occipital Cortex	27.57	−80.26	40.94	441		
Right Orbitofrontal Cortex	−10.91	65.58	−3.88	443	*	
Right Precentral Cortex	47.16	5.84	20.97	817	*	
Right Superior Frontal Cortex	2.67	68.01	9.91	445	*	
Right Superior Frontal Cortex	9.2	53.74	5.06	546	*	
Right Superior Frontal Cortex	13.62	46.34	27.84	554		
Right Superior Parietal Cortex	17.99	−77.64	49.9	406	*	
Right Supramarginal	63.68	−24.54	23.02	533		

* Highlight whether the region is included in the set of top 5 and top 1% EVC values.

Table 3
Statistics of the general linear model for the 4 regions which beta significance were not strongly influenced (changes less than 5%) by the inclusion of the amount of head motion as covariate. Dependent variable: total CBCL score; main regressor: EVC rank; nuisance variables: gender, age and mean frame-displacement.

Brain Region	Site 1		Site 2	
	Beta	p-value	Beta	p-value
Left Superior Frontal Cortex	−14.57	0.03	6.24	0.28
Right Superior Frontal Cortex	7.97	0.25	9.97	0.08
Right Intraparietal Cortex	**−16.14**	**0.02**	**−12.84**	**0.03**
Right Orbitofrontal	−8.50	0.20	1.53	0.78

The values in BOLD highlight the regions with p-values less than 5%.

a pediatric sample, this result might be explored as a potential feature that could be used to identify risk factors in children and adolescents. Moreover, our sample is a community sample based on a non-European/North American population from a developing country, for which relatively few studies exist.

Disclosures and conflict of interest

João R. Sato, Euripedes C. Miguel and Andrea P. Jackowsky are supported by grants from the São Paulo Research Foundation (FAPESP).

Ary Gadelha receives support from a CAPES post-doctoral fellowship and declares no potential conflicts of interest related to the current study.

Felipe Almeida Picon receives support from a CAPES PhD fellowship and declares no potential conflicts of interest.

André Zugman Picon receives support from a CAPES PhD fellowship with no direct conflict of interest with the making of this article.

Giovanni A. Salum receives support from a FAPERGS/CAPES post-doctoral fellowship and declares no potential conflicts of interest.

Pedro Mario Pan receives support from a CNPq PhD fellowship and declares no potential conflicts of interest.

Dr. Edson Amaro Jr has received research grants from FAPESP, CNPq, CAPES, Fundação E.J. Safra and Fundação ABAHDS.

Dr. Luis Augusto Rohde is supported by grants from CNPq and has been on the speakers' bureau/advisory board and/or acted as a consultant for Eli-Lilly, Janssen-Cilag, Novartis and Shire in the last three years. The ADHD and Juvenile Bipolar Disorder Outpatient Programs he chaired received unrestricted educational and research support from the following pharmaceutical companies in the last three years: Eli-Lilly, Janssen-Cilag, Novartis, and Shire. He receives authorship royalties from Oxford Press and ArtMed. He has also received travel awards from Shire for his participation in the 2014 APA and 2015 WFADHD meetings.

Dr. Rodrigo A. Bressan has been on the speakers' bureau/advisory board of AstraZeneca, Bristol, Janssen and Lundbeck and has received research grants from Janssen, Eli Lilly, Lundbeck, Novartis, Roche, FAPESP, CNPq, CAPES, Fundação E.J. Safra and Fundação ABAHDS. He is a shareholder of Biomolecular Technology Ltd.

All of the other authors report no biomedical financial interests or potential conflicts of interest.

Acknowledgements

The opinions, hypotheses, conclusions and recommendations of this study are those of the authors and do not necessary represent the opinions of the funding agencies. The authors are grateful to Sao Paulo Research Foundation - FAPESP (J.R.S. grants 2013/10498-6 and 2013/00506-1; A.P.J. grant 2013/08531-5) for funding this research. This is a study from the National Institutes of Science and Technology for Developmental Psychiatry of Children and Adolescents (INPD) supported by CNPq (573974/2008-0 and 442026/2014-5) and FAPESP (2008/57896-8). A.G., A.Z., F.A.P. and G.A.S. receive fellowships from CAPES-Brazil. P.M.P. receives a fellowship from CNPq-Brazil.

References

ABIPEME, 2010. Associação Brasileira de Empresas de Pesquisa (ABEP), Critério de Classificação Econômica Brasil São Paulo: ABEP.

Achenbach, T., Rescorla, L., 2001. Manual for the ASEBA school-age forms & profiles: an integrated system of multi-informant assessment. University of Vermont Research Center for Children, Youth, & Families, Burlington, VT.

Albert, R., Jeong, H., Barabasi, A.L., 2000. Error and attack tolerance of complex networks? Nature 406 (6794), 378–382.

Andrews-Hanna, J.R., Reidler, J.S., Sepulcre, J., Poulin, R., Buckner, R.L., 2010. Functional-anatomic fractionation of the brain's default network. Neuron 65, 550–562.

Baird, B., Smallwood, J., Gorgolewski, K.J., Margulies, D.S., 2013. Medial and lateral networks in anterior prefrontal cortex support metacognitive ability for memory and perception. J. Neurosci. 33, 16657–16665.
Betzel, R.F., Byrge, L., He, Y., Goñi, J., Zuo, X.N., Sporns, O., 2014. Changes in structural and functional connectivity among resting-state networks across the human lifespan? Neuroimage 102 (2), 345–357.
Biazoli Jr., C.E., Sturzbecher, M., White, T.P., dos Santos Onias, H.H., Andrade, K.C., de Araujo, D.B., Sato, J.R., 2013. Application of partial directed coherence to the analysis of resting-state EEG-fMRI data. Brain Connect. 3 (6), 563–568.
Binder, J.R., Desai, R.H., Graves, W.W., Conant, L.L., 2009. Where is the semantic system? A critical review and meta-analysis of 120 functional neuroimaging studies. Cereb. Cortex 19, 2767–2796.
Bleich-Cohen, M., Jamshy, S., Sharon, H., Weizman, R., Intrator, N., Poyurovsky, M., Hendler, T., 2014. Machine learning fMRI classifier delineates subgroups of schizophrenia patients. Schizophr. Res. 160 (1), 196–200.
Bonacich, P., 1987. Power and centrality: a family of measures. Am. J. Sociol., 1170–1182.
Buckner, R.L., Andrews-Hanna, J.R., Schacter, D.L., 2008. The brain's default network. Ann. N. Y. Acad. Sci. 1124, 1–38.
Buckner, R.L., Sepulcre, J., Talukdar, T., Krienen, F.M., Liu, H., Hedden, T., Andrews-Hanna, J.R., Sperling, R.A., Johnson, K.A., 2009. Cortical hubs revealed by intrinsic functional connectivity: mapping, assessment of stability, and relation to Alzheimer's disease. J. Neurosci. 29, 1860–1873.
Cox, R.W., 1996. AFNI: software for analysis and visualization of functional magnetic resonance neuroimages. Comput. Biomed. Res. 29, 162–173.
Crossley, N.A., Mechelli, A., Scott, J., Carletti, F., Fox, P.T., McGuire, P., Bullmore, E.T., 2014. The hubs of the human connectome are generally implicated in the anatomy of brain disorders. Brain 137, 2382–2395.
Di Martino, A., Fair, D.A., Kelly, C., Satterthwaite, T.D., Castellanos, F.X., Thomason, M.E., Craddock, R.C., Luna, B., Leventhal, B.L., Zuo, X.-N., 2014. Unraveling the miswired connectome: a developmental perspective. Neuron 83, 1335–1353.
Dosenbach, N.U., Fair, D.A., Miezin, F.M., Cohen, A.L., Wenger, K.K., Dosenbach, R.A., Petersen, S.E., 2007. Distinct brain networks for adaptive and stable task control in humans. Proc. Natl. Acad. Sci. 104 (26), 11073–11078.
dos Santos Siqueira, A., Biazoli Junior, C.E., Comfort, W.E., Rohde, L.A., Sato, J.R., 2014. Abnormal functional resting-State networks in ADHD: graph theory and pattern recognition analysis of fMRI data. BioMed Res. Int. 2014.
Fair, D.A., Dosenbach, N.U., Church, J.A., Cohen, A.L., Brahmbhatt, S., Miezin, F.M., Barch, D.M., Raichle, M.E., Petersen, S.E., Schlaggar, B.L., 2007. Development of distinct control networks through segregation and integration. Proc. Natl. Acad. Sci. 104, 13507–13512.
Fair, D.A., Cohen, A.L., Dosenbach, N.U., Church, J.A., Miezin, F.M., Barch, D.M., Raichle, M.E., Petersen, S.E., Schlaggar, B.L., 2008. The maturing architecture of the brain's default network. Proc. Natl. Acad. Sci. U. S. A. 105, 4028–4032.
Fair, D.A., Cohen, A.L., Power, J.D., Dosenbach, N.U., Church, J.A., Miezin, F.M., Schlaggar, B.L., Petersen, S.E., 2009. Functional brain networks develop from a local to distributed organization. PLoS Comput. Biol. 5, e1000381.
Fornito, A., Zalesky, A., Breakspear, M., 2015. The connectomics of brain disorders. Nat. Rev. Neurosci. 16, 159–172.
Fox, M.D., Snyder, A.Z., Vincent, J.L., Corbetta, M., Van Essen, D.C., Raichle, M.E., 2005. The human brain is intrinsically organized into dynamic: anticorrelated functional networks. Proc. Natl. Acad. Sci. U. S. A. 102 (27), 9673–9678.
Fransson, P., Åden, U., Blennow, M., Lagercrantz, H., 2011. The functional architecture of the infant brain as revealed by resting-state fMRI. Cereb. Cortex 21, 145–154.
Gao, W., Zhu, H., Giovanello, K.S., Smith, J.K., Shen, D., Gilmore, J.H., Lin, W., 2009. Evidence on the emergence of the brain's default network from 2-week-old to 2-year-old healthy pediatric subjects. Proc. Natl. Acad. Sci. 106, 6790–6795.
Gong, G., He, Y., Concha, L., Lebel, C., Gross, D.W., Evans, A.C., Beaulieu, C., 2009. Mapping anatomical connectivity patterns of human cerebral cortex using in vivo diffusion tensor imaging tractography. Cereb. Cortex 19, 524–536.
Grayson, D.S., Ray, S., Carpenter, S., Iyer, S., Dias, T.G.C., Stevens, C., Nigg, J.T., Fair, D.A., 2014. Structural and functional rich club organization of the brain in children and adults. PLoS One 9, e88297.
Hagmann, P., Cammoun, L., Gigandet, X., Meuli, R., Honey, C.J., Wedeen, V.J., Sporns, O., 2008. Mapping the structural core of human cerebral cortex. PLoS Biol. 6, e159.
He, Y., Xu, T., Zhan, W., Zuo, X., 2016. Lifespan anxiety is reflected in human amygdala cortical connectivity. Hum. Brain Mapp. 37 (March (3)), 1178–1193, http://dx.doi.org/10.1002/hbm.23094, Epub 2015 December.
Hellyer, P.J., Shanahan, M., Scott, G., Wise, R.J., Sharp, D.J., Leech, R., 2014. The control of global brain dynamics: opposing actions of frontoparietal control and default mode networks on attention? J. Neurosci. 34 (2), 451–461.
Horga, G., Kaur, T., Peterson, B.S., 2014. Annual research review: current limitations and future directions in MRI studies of child- and adult-onset developmental psychopathologies? J. Child Psychol. Psychiatry 55 (6), 659–680.
Hwang, K., Hallquist, M.N., Luna, B., 2013. The development of hub architecture in the human functional brain network. Cereb. Cortex 23, 2380–2393.
Jacobs, H.I., Van Boxtel, M.P., Heinecke, A., Gronenschild, E.H., Backes, W.H., Ramakers, I.H., Jolles, J., Verhey, F.R., 2012. Functional integration of parietal lobe activity in early Alzheimer disease. Neurology 78, 352–360.
Jenkinson, M., Beckmann, C.F., Behrens, T.E., Woolrich, M.W., Smith, S.M., 2012. Fsl. Neuroimage, 62, 782–790.
Khundrakpam, B.S., Reid, A., Brauer, J., Carbonell, F., Lewis, J., Ameis, S., Karama, S., Lee, J., Chen, Z., Das, S., 2013. Developmental changes in organization of structural brain networks. Cereb. Cortex 23, 2072–2085.
Markett, S., Reuter, M., Montag, C., Voigt, G., Lachmann, B., Rudorf, S., Weber, B., 2014. Assessing the function of the fronto-parietal attention network: insights from resting-state fMRI and the attentional network test. Hum. Brain Mapp. 35 (4), 1700–1709.
Medvedev, A.V., 2014. Does the resting state connectivity have hemispheric asymmetry? A near-infrared spectroscopy study. Neuroimage 85, 400–407.
Patel, A.X., Kundu, P., Rubinov, M., Jones, P.S., Vértes, P.E., Ersche, K.D., Suckling, J., Bullmore, E.T., 2014. A wavelet method for modeling and despiking motion artifacts from resting-state fMRI time series. Neuroimage 95, 287–304.
Power, J.D., Barnes, K.A., Snyder, A.Z., Schlaggar, B.L., Petersen, S.E., 2012. Spurious but systematic correlations in functional connectivity MRI networks arise from subject motion. Neuroimage 59, 2142–2154.
Power, J.D., Schlaggar, B.L., Lessov-Schlaggar, C.N., Petersen, S.E., 2013. Evidence for hubs in human functional brain networks. Neuron 79, 798–813.
Rademacher, J., Galaburda, A., Kennedy, D., Filipek, P., Caviness, V., 1992. Human cerebral cortex: localization, parcellation, and morphometry with magnetic resonance imaging. Cogn. Neurosci. J. 4, 352–374.
Raichle, M.E., Snyder, A.Z., 2007. A default mode of brain function: a brief history of an evolving idea. Neuroimage 37, 1083–1090.
Raichle, M.E., MacLeod, A.M., Snyder, A.Z., Powers, W.J., Gusnard, D.A., Shulman, G.L., 2001. A default mode of brain function. Proc. Natl. Acad. Sci. 98, 676–682.
Ray, S., Miller, M., Karalunas, S., Robertson, C., Grayson, D.S., Cary, R.P., Hawkey, E., Painter, J.G., Kriz, D., Fombonne, E., 2014. Structural and functional connectivity of the human brain in autism spectrum disorders and attention-deficit/hyperactivity disorder: a rich club-organization study. Hum. Brain Mapp. 35, 6032–6048.
Rubinov, M., Sporns, O., 2010. Complex network measures of brain connectivity: uses and interpretations. Neuroimage 52 (3), 1059–1069.
Sack, A.T., 2009. Parietal cortex and spatial cognition. Behav. Brain Res. 202, 153–161.
Saenger, V.M., Barrios, F.A., Martínez-Gudiño, M.L., Alcauter, S., 2012. Hemispheric asymmetries of functional connectivity and grey matter volume in the default mode network. Neuropsychologia 50 (7), 1308–1315.
Salum, G.A., Mogg, K., Bradley, B.P., Gadelha, A., Pan, P., Tamanaha, A.C., Moriyama, T., Graeff-Martins, A.S., Jarros, R.B., Polanczyk, G., do Rosario, M.C., Leibenluft, E., Rohde, L.A., Manfro, G.G., Pine, D.S., 2013. Threat bias in attention orienting: evidence of specificity in a large community-based study. Psychol. Med. 43, 733–745.
Salum, G.A., Gadelha, A., Pan, P.M., Moriyama, T.S., Graeff-Martins, A.S., Tamanaha, A.C., Alvarenga, P., Krieger, F.V., Fleitlich-Bilyk, B., Jackowski, A., 2014. High risk cohort study for psychiatric disorders in childhood: rationale, design, methods and preliminary results. Int. J. Method Psychiatr. Res.
Sato, J.R., Salum, G.A., Gadelha, A., Vieira, G., Zugman, A., Picon, F.A., Pan, P.M., Hoexter, M.Q., Anés, M., Moura, L.M., 2015a. Decreased centrality of subcortical regions during the transition to adolescence: a functional connectivity study. Neuroimage 104, 44–51.
Sato, J.R., Biazoli Jr., C.E., Salum, G.A., Gadelha, A., Crossley, N., Satterthwaite, T.D., Vieira, G., Zugman, A., Picon, F.A., Pan, P.M., Hoexter, M.Q., Anés, M., Moura, L.M., Del'aquilla, M.A., Amaro Jr., E., McGuire, P., Lacerda, A.L., Rohde, L.A., Miguel, E.C., Jackowski, A.P., Bressan, R.A., 2015b. Temporal stability of network centrality in control and default mode networks: specific associations with externalizing psychopathology in children and adolescents? Hum. Brain Mapp. 36 (12), 4926–4937.
Satterthwaite, T.D., Baker, J.T., 2015. How can studies of resting-state functional connectivity help us understand psychosis as a disorder of brain development? Curr. Opin. Neurobiol. 30, 85–91.
Seeley, W.W., Menon, V., Schatzberg, A.F., Keller, J., Glover, G.H., Kenna, H., Greicius, M.D., 2007. Dissociable intrinsic connectivity networks for salience processing and executive control. J. Neurosci. 27 (9), 2349–2356.
Seghier, M.L., 2013. The angular gyrus multiple functions and multiple subdivisions. Neuroscientist 19, 43–61.
Singh-Curry, V., Husain, M., 2009. The functional role of the inferior parietal lobe in the dorsal and ventral stream dichotomy. Neuropsychologia 47, 1434–1448.
Sporns, O., Honey, C.J., Kötter, R., 2007. Identification and classification of hubs in brain networks. PLoS One 2, e1049.
Sporns, O., 2014. Towards network substrates of brain disorders. Brain 137, 2117–2118.
Spreng, R.N., Mar, R.A., Kim, A.S., 2009. The common neural basis of autobiographical memory, prospection, navigation, theory of mind, and the default mode: a quantitative meta-analysis. J. Cogn. Neurosci. 21, 489–510.
Supekar, K., Musen, M., Menon, V., 2009. Development of large-scale functional brain networks in children. PLoS Biol. 7, e1000157.
Supekar, K., Uddin, L.Q., Prater, K., Amin, H., Greicius, M.D., Menon, V., 2010. Development of functional and structural connectivity within the default mode network in young children. Neuroimage 52, 290–301.
Tellegen, A., Briggs, P.F., 1967. Old wine in new skins: grouping Wechsler subtests into new scales. J. Consult. Psychol. 31, 499.
Thaler, A., Mirelman, A., Helmich, R.C., van Nuenen, B.F., Rosenberg-Katz, K., Gurevich, T., Orr-Urtreger, A., Marder, K., Bressman, S., Bloem, B.R., Giladi, N., Hendler, T., 2013. Neural correlates of executive functions in healthy G2019S LRRK2 mutation carriers. Cortex 49, 2501–2511.
Tomasi, D., Volkow, N.D., 2014. Mapping small-world properties through development in the human brain: disruption in schizophrenia. PLoS One 9, e96176.

Uddin, L.Q., Supekar, K.S., Ryali, S., Menon, V., 2011. Dynamic reconfiguration of structural and functional connectivity across core neurocognitive brain networks with development. J. Neurosci. 31, 18578–18589.
van den Heuvel, M.P., Sporns, O., 2013. Network hubs in the human brain. Trends Cogn. Sci. 17, 683–696.
Vigneau, M., Beaucousin, V., Herve, P.-Y., Duffau, H., Crivello, F., Houde, O., Mazoyer, B., Tzourio-Mazoyer, N., 2006. Meta-analyzing left hemisphere language areas: phonology, semantics, and sentence processing. Neuroimage 30, 1414–1432.
Wang, Y., Hamilton, A.F.d.C., 2014. Anterior medial prefrontal cortex implements social priming of mimicry. Soc. Cogn. Affect. Neurosci. 10 (April (4)), 486–493, http://dx.doi.org/10.1093/scan/nsu076, Epub 2014 July.
Weissman, M.M., Wickramaratne, P., Adams, P., Wolk, S., Verdeli, H., Olfson, M., 2000. Brief screening for family psychiatric history: the family history screen. Arch. Gen. Psychiatry 57 (7), 675–682.
Zalesky, A., 2011. Moderating registration misalignment in voxelwise comparisons of DTI data: a performance evaluation of skeleton projection. Magn. Reson. Imaging 29, 111–125.
Zuo, X.-N., Ehmke, R., Mennes, M., Imperati, D., Castellanos, F.X., Sporns, O., Milham, M.P., 2012. Network centrality in the human functional connectome. Cereb. Cortex 22, 1862–1875.
Zysset, S., Huber, O., Samson, A., Ferstl, E.C., von Cramon, D.Y., 2003. Functional specialization within the anterior medial prefrontal cortex: a functional magnetic resonance imaging study with human subjects. Neurosci. Lett. 335, 183–186.